Research article

GEEA
Geochemistry: Exploration, Environment, Analysis

https://doi.org/10.1144/geochem2023-007 | Vol. 23 | 2023 | geochem2023-007

Anthropogenic influence on groundwater geochemistry in Horn Creek Watershed near the Orphan Mine in Grand Canyon National Park, Arizona, USA

Kimberly R. Beisner[1]*, Collin Davidson[2] and Fred Tillman[3]

[1] U.S. Geological Survey, 6700 Edith Blvd. NE, Albuquerque, NM 87111, USA
[2] University of Nevada Las Vegas, NV, USA
[3] U.S. Geological Survey, Tucson, AZ 85719, USA
KRB, 0000-0002-2077-6899; CD, 0000-0001-8814-9982; FT, 0000-0002-2922-402X
* Correspondence: kbeisner@usgs.gov

Abstract: Breccia pipe deposits of the Grand Canyon region contain ore grade copper and uranium. Horn Creek is located near the Orphan Mine mineralized breccia pipe deposit, and groundwater emerging from the bedrock in the headwaters of Horn Creek has the highest uranium concentrations in the region. Uranium decreases an order of magnitude between the groundwater at the top of the watershed and the groundwater emerging from the alluvial material lower in the watershed. Horn Creek water has low sulfur and uranium isotopic ratios which may suggest interaction with sulfide and uranium minerals found in mineralized breccia pipe deposits. Per- and polyfluoroalkyl substances were found in low concentrations in groundwater from the bedrock and may be related to mining process materials or other anthropogenic activities. PHREEQC modelling suggests that water that is elevated in uranium emerging from the bedrock in the upper watershed may mix with other groundwater and atmospheric precipitation infiltrated into the alluvial material in the lower watershed. Tritium is elevated in Horn Creek groundwaters, suggesting a component of modern water, some of which may have interacted with Orphan Mine workings. Additional studies could build on this understanding of chemistry changes in the waters of Horn Creek to provide more direct evidence of the contribution of water moving through the Orphan Mine.

Keywords: uranium mining; isotope geochemistry; Grand Canyon; anthropogenic

Supplementary material: Chemical data for this paper are available at https://doi.org/10.5066/F7P55KJN, PHREEQC geochemical simulations are available at https://doi.org/10.5066/P9X17FKG and groundwater chemistry from south of Grand Canyon, AZ is available at https://doi.org/10.6084/m9.figshare.c.6747638

Thematic collection: This article is part of the Geochemical processes related to mined, milled, or natural metal deposits collection available at: https://www.lyellcollection.org/topic/collections/geochemical-processes-related-to-mined-milled-or-natural-metal-deposits

Received 18 January 2023; **revised** 30 June 2023; **accepted** 7 July 2023

The Grand Canyon region hosts some of the highest-grade uranium ore in the United States (Alpine and Brown 2010). In 1951, uranium ore was discovered in the Orphan copper mine west of Grand Canyon Village (Fig. 1), initiating the era of uranium exploration and mining in the area (Chenoweth 1986). In 2009, uranium prices increased, resulting in a large number of mining claims in the Grand Canyon region that led the U.S. Secretary of the Interior to initiate a two year withdrawal of about one million acres of Federal land from future mineral entry (Alpine and Brown 2010). The withdrawal was extended for 20 years in 2012 subject to valid existing rights. Since 2012, the U.S. Geological Survey (USGS) has been conducting scientific investigations to understand effects from breccia pipe uranium mining in the Grand Canyon region. This study focuses on the Horn Creek watershed as a case study for water resources near a former breccia pipe uranium mine (Orphan Mine).

The former Orphan Mine is located at the head of the eastern branch of the Horn Creek watershed. The Orphan Mine is completed within a breccia pipe deposit that was mined from 1893 to 1951 as a copper mine, and then in 1951 uranium ore was discovered in the mining material, and the breccia pipe was mined for uranium from 1953 to 1969 (Chenoweth 1986). The mine was turned over to the National Park Service in 1987 and remains as it was at the end of the mining period (Chenoweth 1986). Estimates suggest approximately four million pounds of uranium oxide remain in the breccia pipe beneath the mine workings (Chenoweth 1986). Vertical and horizontal shafts were drilled into the breccia pipe ore deposit at the Orphan Mine to extract ore material, and mine waste was placed back into the mine void spaces (Chenoweth 1986). Additionally, 13 exploratory holes were drilled from the lowest mine working level to the depth of the Tapeats Sandstone below the mine, the deepest of which (P-13) is 583 m below the mine workings, which is the depth of the Tapeats Sandstone below the mine (Fig. 2; Chenoweth 1986). An opening in the rock roof above the mine workings is present at the stratigraphic level of the Coconino Sandstone that connects the atmosphere to underground mine workings and continues to collapse and widen (Fig. 2). Water seeps out of mine shafts near the opening in the rock roof, but little is known about the presence and depth of water in deeper mine workings of the Orphan Mine.

Hydrogeologic setting

Horn Creek is a branched watershed tributary to the Colorado River in Grand Canyon (Fig. 1a). Water emerges from the upper reaches of the Horn Creek watershed in the eastern branch at the base of bedrock cliffs below the Redwall Limestone and above the Muav Limestone. This spring water disappears and then re-emerges from alluvial material lower in the Horn Creek watershed. Streamflow in

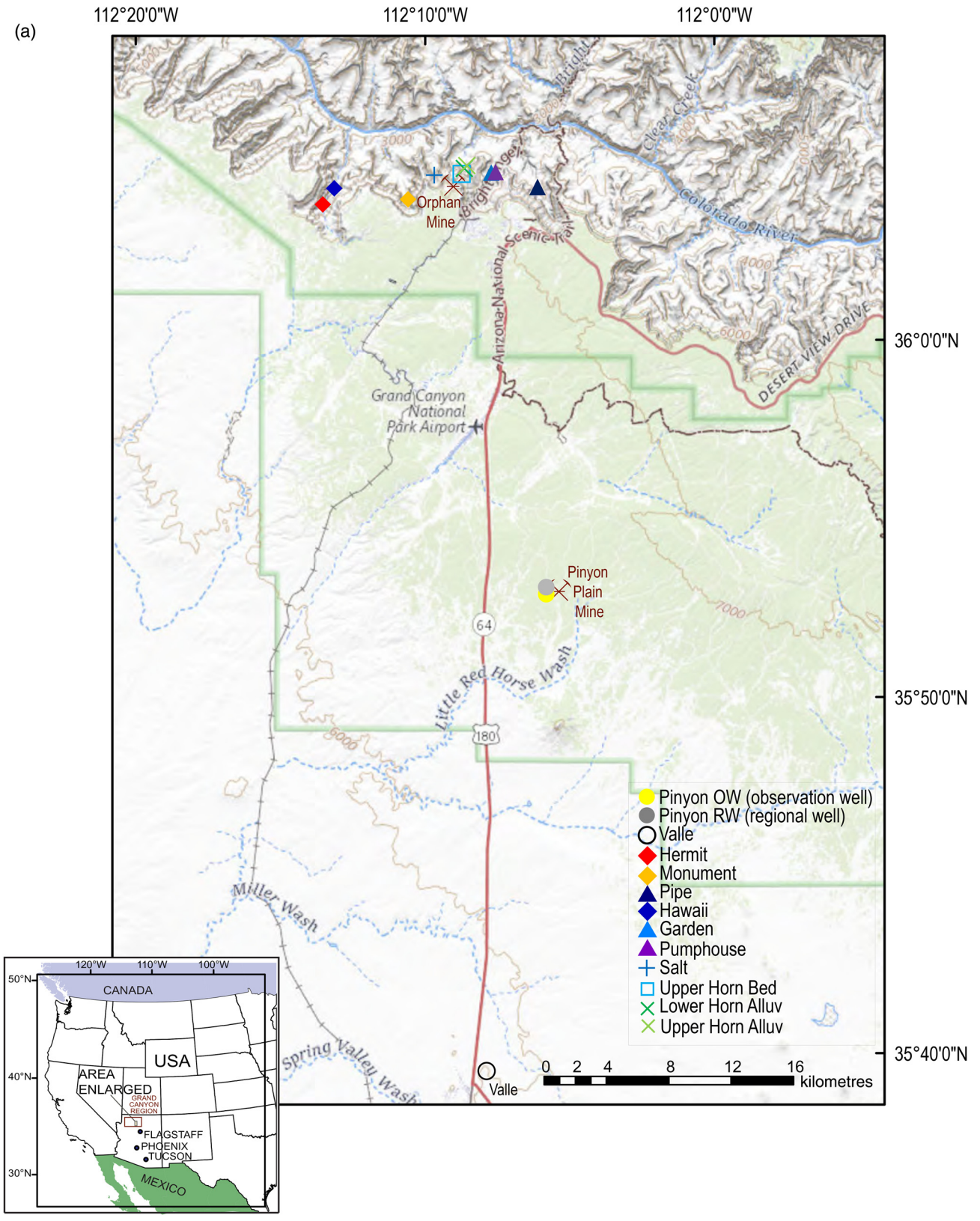

Fig. 1. (**a**) Map of groundwater sample locations and breccia pipe uranium mines south of Grand Canyon with (**b**) a map showing detail of the Horn Creek watershed sampling locations where solid blue lines represent the approximate location of perennial flow in Horn Creek below spring sites in this study, dashed blue lines represent ephemeral flow and the black line represents the fault expression, with geology from Billingsley (2000) and base map from USGS The National Map.

the west branch of the Horn Creek watershed also begins from water emerging from near the base of the bedrock cliffs high in the watershed and re-emerges lower from alluvial material but is lower in volume compared with the eastern branch and is not included in this study.

Fitzgerald (1996) documented one elevated uranium concentration of 92.7 µg l^{-1} from a Horn Creek sample in 1995, which was collected by going up watershed from previous sampling in the lower alluvial pool, which had observed uranium concentrations of 24.7 and 27.6 µg l^{-1}. Liebe (2003) published the highest

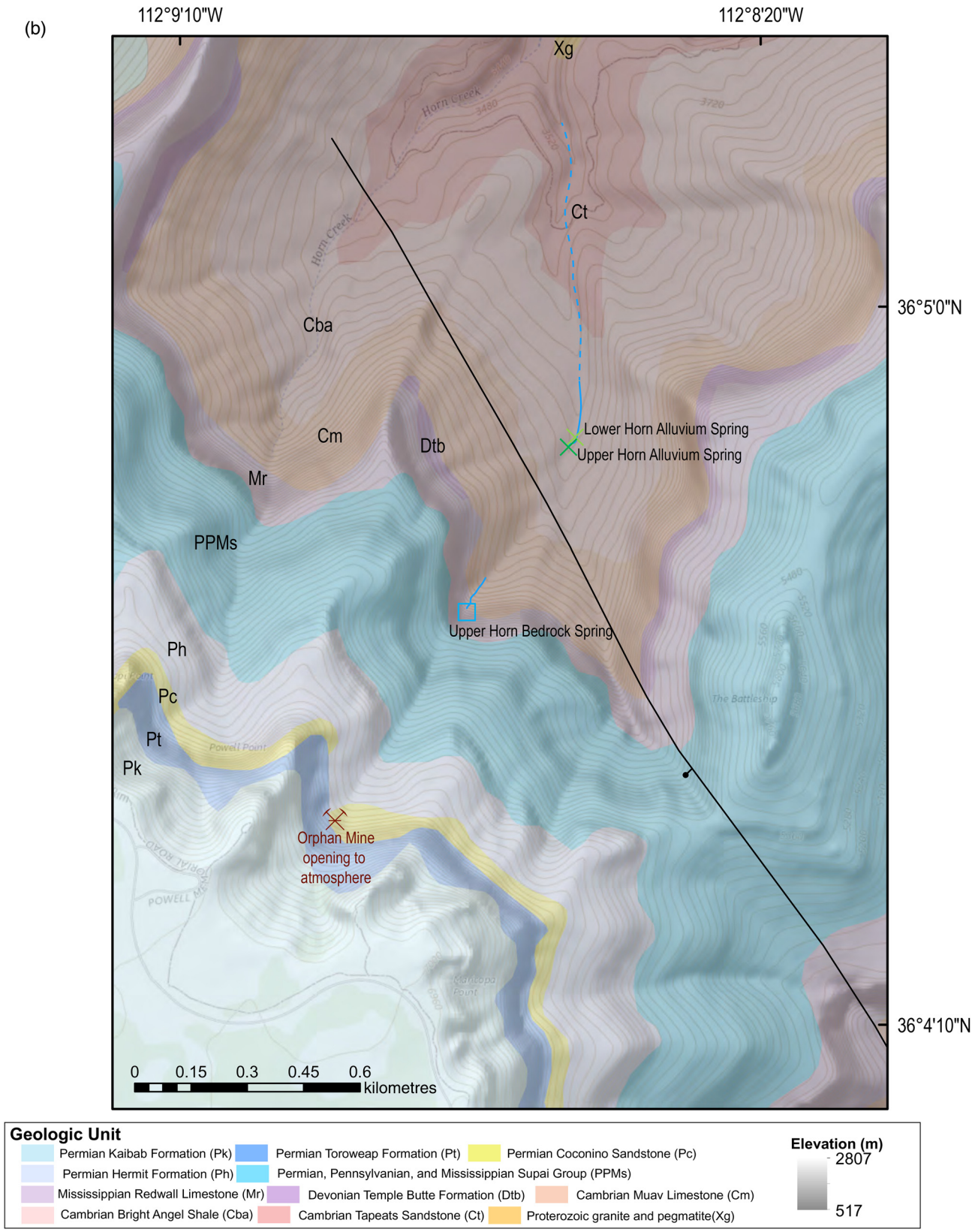

Fig. 1. Continued.

uranium concentrations from sites in Horn Creek (400 µg l^{-1}), collected at the highest location accessible by foot in the watershed at the bottom of the Redwall Limestone cliff face. The current study includes samples collected by the USGS from the eastern Horn Creek watershed including the uppermost spring in the Horn watershed (2018–22), as well as samples collected at springs emerging from alluvial material lower in the watershed (2000–22). This study assesses the geochemical tracers from Horn Creek water samples related to other nearby groundwater to determine anthropogenic changes and utilizes PHREEQC modelling to understand possible chemical interactions that are occurring in waters of Horn Creek.

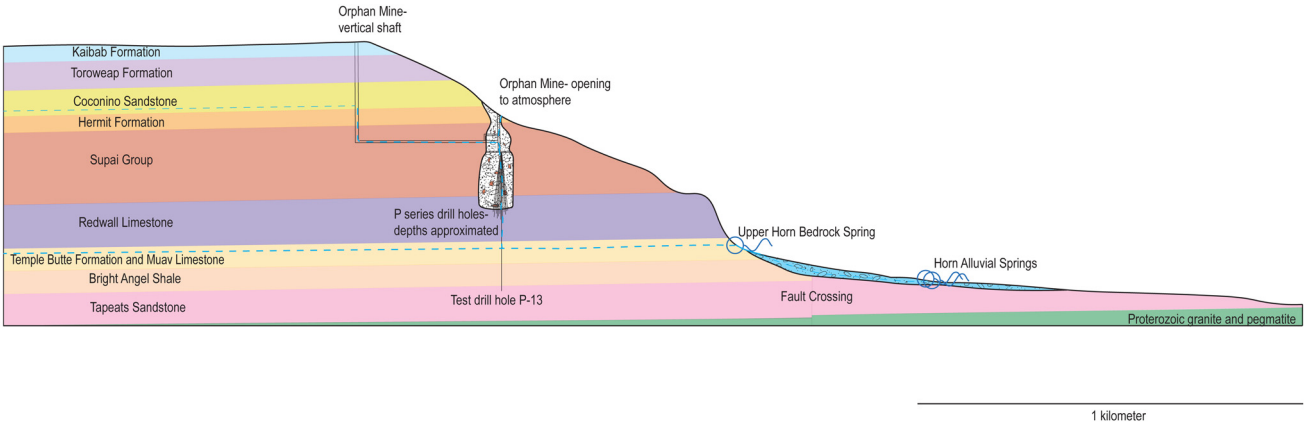

Fig. 2. Generalized schematic down the eastern branch of Horn Creek (Fig. 1b) including the Orphan Mine breccia pipe deposit and mine workings. Dashed blue lines show conceptual understanding of groundwater resources in the region and how they may interact with the Orphan Mine workings.

Methods

Water samples were collected for this study from spring sites between April 2018 and April 2022. The analytical results were combined with reported data published in Monroe *et al.* (2005) and Bills *et al.* (2007). All samples were collected by the USGS using standard field methods (U.S. Geological Survey variously dated). Major ions and trace element samples, nutrients, radiocarbon, isotopes of strontium, uranium and sulfate were filtered through a 0.45 µm capsule filter. Tritium, per- and polyfluoroalkyl substances (PFAS) and stable isotopes of oxygen and hydrogen samples were not filtered. PFAS samples were collected while wearing elbow-length gloves and using non-waterproof bottle labels written with ballpoint pen. Detailed field and analytical descriptions are published in Beisner *et al.* (2017).

Field parameters including pH, water temperature, specific conductance, dissolved oxygen and barometric pressure were measured on site just before water samples were collected. Spring samples were collected as close to the point of issuance from the ground as possible using a peristaltic pump with flexible silicon tubing. PFAS samples were collected directly into 2–250 ml polycarbonate bottles and kept chilled until analysis.

Alkalinity was measured in the field within four hours of sample collection using the inflection point titration method. Water samples were analysed for major, trace and rare-earth elements by the USGS Integrated Water Chemistry Analytical Laboratory (IWCAL) in Boulder, CO (USGSTMCO) using methods from Garbarino and Taylor (1979, 1996) and Taylor (2001). The precision for all methods analysed by the IWCAL was 4% or better depending on the element. PFAS samples were analysed at SGS Orlando using the EPA modified 537.1 method (Shoemaker and Tettenhorst 2018).

Strontium isotope ratios ($^{87}Sr/^{86}Sr$) were measured by the USGS National Research Program Laboratory in Menlo Park, CA, using methods described in Bullen *et al.* (1996) with precision of ±0.00002 or better at the 95% confidence level. ALS Environmental in Fort Collins, CO, under contract to the USGS, analysed water

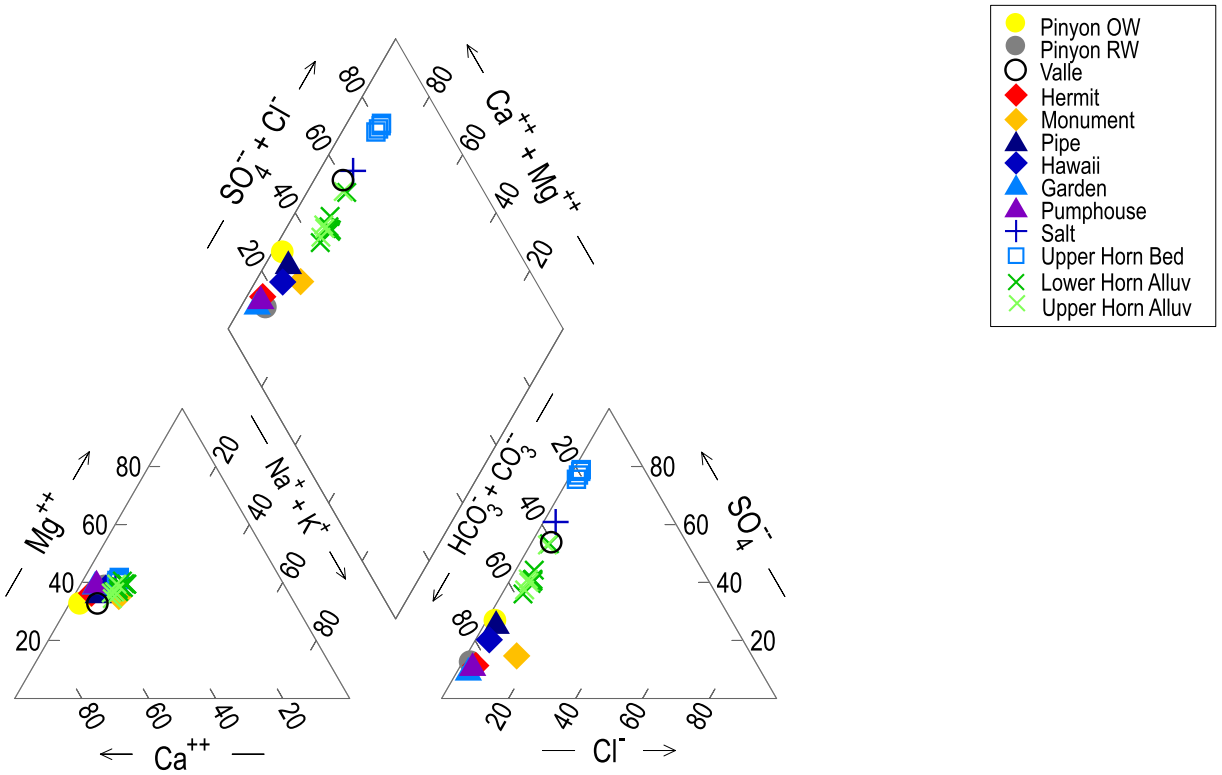

Fig. 3. Piper plot of major ion proportion for groundwater samples; values presented in per cent.

Table 1. *Select trace element concentrations from Horn Creek samples*

USGS Site Number	Sample Date	Common Name	Cl (mg l^{-1})	As	Ba	Mo	Rb	Se	Sr	U	Zn
360439112084601	5/1/18 15:15	Upper Horn Bed	18	5.3	23	11	15	15	446	257	.9
360439112084601	4/18/19 11:00	Upper Horn Bed	17.3	5.5	24	10	14	13	404	195	.4
360439112084601	6/2/20 17:30	Upper Horn Bed	17.8	5.3	25	11	15	12	446	293	2.2
360439112084601	11/3/21 11:30	Upper Horn Bed	–	5.5	271	12	9.7	14	438	228	–
360439112084601	12/22/21 11:45	Upper Horn Bed	–	5.7	235	12	10	14	437	231	–
360439112084601	4/20/22 16:00	Upper Horn Bed	19	6.3	31	12	15	14	440	236	4.7
360449112083701	5/1/18 11:15	Upper Horn Alluv	32	2.9	43	5.1	6.6	7.2	242	23	.8
360449112083701	4/16/19 13:00	Upper Horn Alluv	30.6	2.4	47	6.4	6.6	7.8	250	34	.6
360449112083701	6/2/20 19:30	Upper Horn Alluv	31.7	7.7	54	5.4	6.7	–	247	26	.6
360449112083701	11/3/21 11:00	Upper Horn Alluv	–	3	434	5	4.3	6.1	257	22	–
360449112083701	12/22/21 11:00	Upper Horn Alluv	–	2.4	419	4.8	3.5	6.2	229	21	–
360449112083701	4/20/22 17:00	Upper Horn Alluv	32.1	2.7	46	4.9	6.4	7	242	26	2.3
360443112083300	5/1/18 12:00	Lower Horn Alluv	32	2.9	48	2.9	7.4	7.3	252	7.6	1.1
360443112083300	4/16/19 12:15	Lower Horn Alluv	31.3	2.9	51	3.6	7.3	7.7	273	14	.7

Data from the U.S. Geological Survey National Water Information System (USGS 2022).
Cl values in mg l^{-1}; other values are in µg l^{-1}; –, not determined.

samples for uranium isotopes (^{234}U, ^{235}U and ^{238}U) using alpha-counting methods (ASTM D 3972). Sulfate isotopes ($\delta^{34}S$ and $\delta^{18}O$ of sulfate) and stable isotopes of water ($\delta^{18}O$ and $\delta^{2}H$) were analysed at the USGS Reston Stable Isotope Laboratory using mass spectrometry following methods by Révész *et al.* (2012) and Révész and Coplen (2008*a*; *b*). Tritium samples collected from 2018 to 2020 were analysed at the USGS Menlo Park Tritium Laboratory using the electrolytic enrichment liquid scintillation counting method (Thatcher *et al.* 1977) with a detection level of 0.5 pCi l^{-1}. The University of Miami Tritium Laboratory, FL, analysed tritium in samples collected in 2021 and 2022 using the electrolytic enrichment and gas-counting method, with a reporting level of 0.3 pCi l^{-1} (Ostlund *et al.* 1969).

PHREEQCI version 3.5.0 (Charlton and Parkhurst 2002; Parkhurst and Appelo 2013) was used to determine saturation indices and run inverse modelling scenarios for water in Horn Creek. The WATEQ4F database (Ball and Nordstrom 1991) was used with the default redox potential (pe) value of 4.

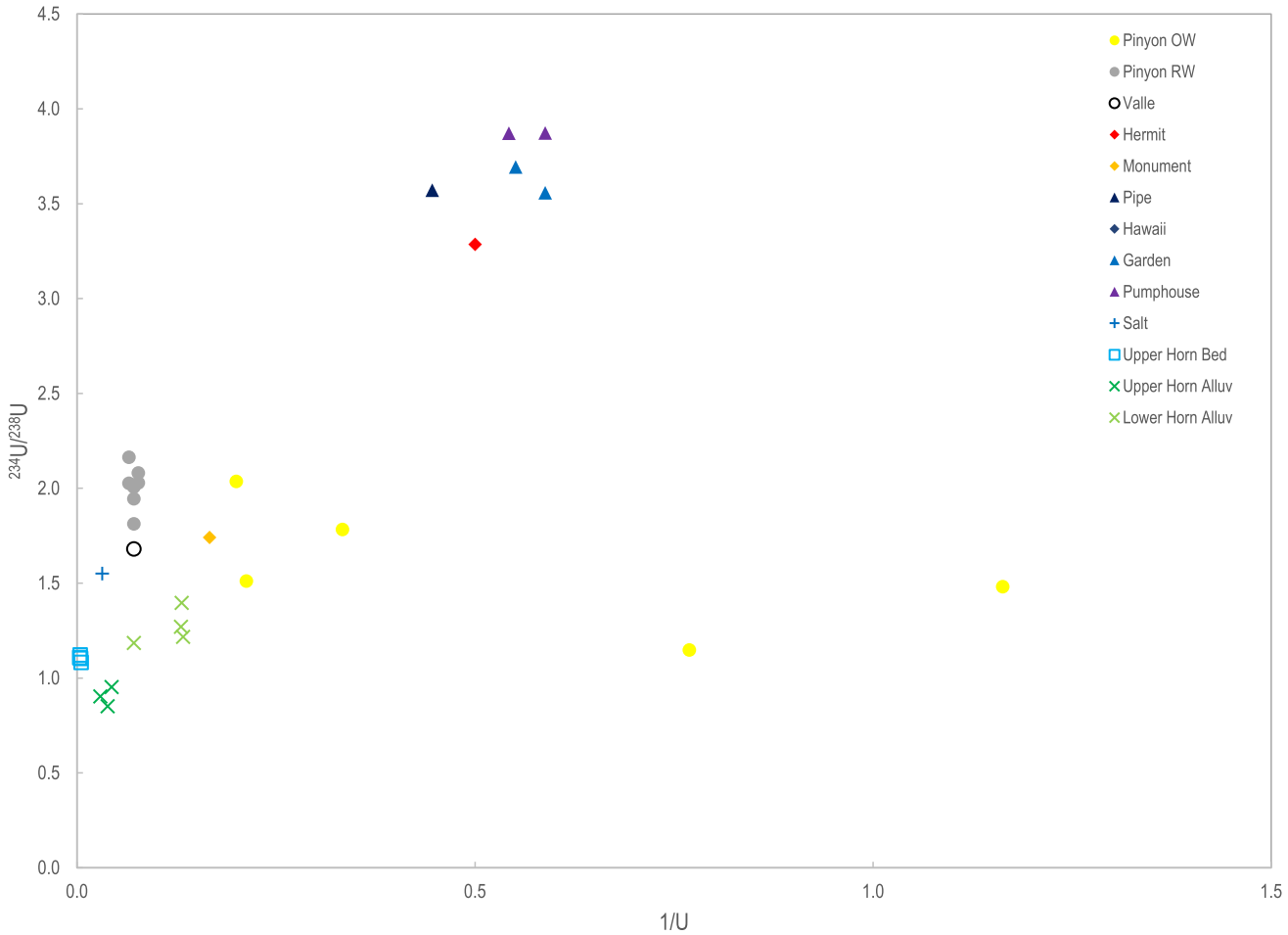

Fig. 4. Uranium activity ratio ($^{234}U/^{238}U$) v. inverse of uranium concentration for groundwater samples.

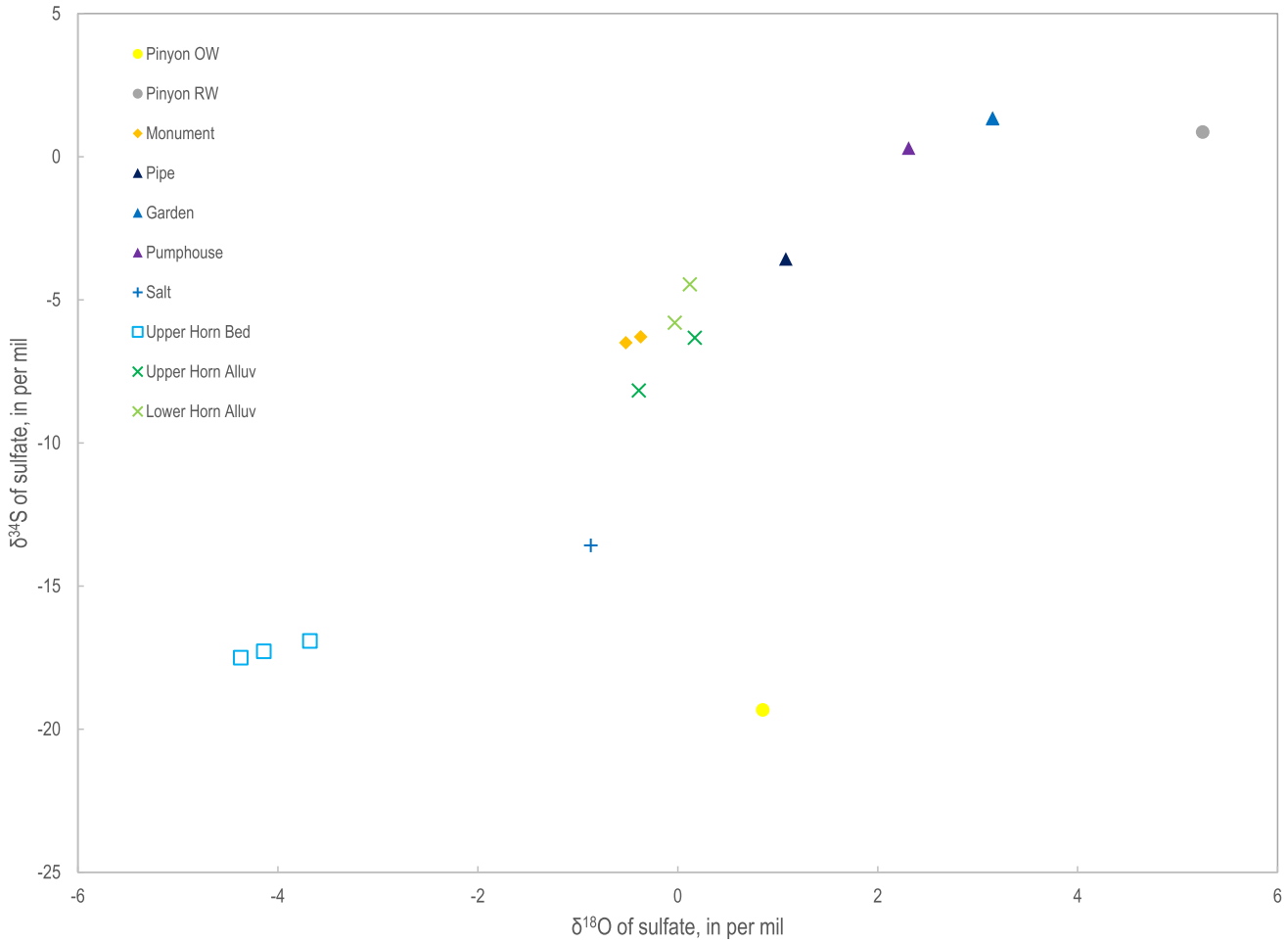

Fig. 5. Sulfur isotopic ratio ($\delta^{34}S$) of sulfate v. oxygen isotopic ratio ($\delta^{18}O$) of sulfate for groundwater samples.

Results

Major and trace element chemistry

Water emerging from a spring near the headwaters of the Horn Creek watershed (Upper Horn Bedrock) were calcium–magnesium sulfate-type waters, whereas those emerging from the alluvial material (Upper and Lower Horn Alluvium) were calcium–magnesium bicarbonate–sulfate-type waters (Fig. 3). The concentrations of calcium, magnesium, sodium and fluoride are similar between the bedrock and alluvial springs, whereas sulfate and potassium are higher at the bedrock spring, and chloride and bicarbonate are higher at the alluvial springs. Other springs in the area have calcium–magnesium bicarbonate-type waters and the Horn alluvial springs and Salt Spring are intermediate between those water types and Horn bedrock (Fig. 3). Water types determined from samples in this study were similar to those of water samples collected from Horn Creek and surrounding springs in 2002 by Liebe (2003).

Several trace elements (arsenic, molybdenum, selenium, strontium, rubidium and uranium) decrease in concentration between the bedrock and alluvial springs. Barium concentrations at Upper Horn Bedrock Spring and Upper Horn Alluvial Spring were elevated in samples collected in November and December 2021. Concentrations at Upper Horn Bedrock Spring were 271 and 235 μg l^{-1} compared to its typical range of 23–31 μg l^{-1} and concentrations were two times higher at Upper Horn Alluvial Spring (434 and 419 μg l^{-1}) compared to its typical range of 43–54 μg l^{-1} (Table 1 and Supplementary Information). Some nearby springs (Pumphouse, Garden, Monument and Hermit) consistently have elevated barium concentrations (in the range of 200–350 μg l^{-1}; Supplementary information), and the elevated values in Horn Creek groundwaters may indicate a short-term change in source water to the spring or other geochemical process that warrants further investigation.

Isotopes

A ratio of uranium isotopes ^{234}U to ^{238}U near 1 indicates secular equilibrium (Faure and Mensing 2005), which is the condition in rock and mineralized deposits. As water interacts with rock and mineralized deposits, the uranium in the water acquires the uranium isotopic ratio of the solid phase. As the water moves farther from the interaction with the source of the uranium, alpha recoil from the surrounding aquifer matrix causes an increase in the uranium isotopic ratio. Springs emerging in the Horn Creek watershed (both bedrock and alluvium) have the lowest uranium isotopic ratios (near 1) suggesting interaction with nearby solid material at secular equilibrium (Fig. 4). Upper Horn Alluvium Spring ranges from 0.85 to 0.95 which is the lowest value from the springs included in this study, suggesting an increase of ^{234}U compared with the Upper Horn Bedrock Spring. Groundwater emerging at Lower Horn Alluvium Spring has higher uranium isotopic ratio values with values closer to other groundwaters of the region (Fig. 4).

Sulfate isotopes at Upper Horn Bedrock Spring have negative values for oxygen and sulfur compared with other groundwater in the region (Fig. 5). The Pinyon Plain Observation Well (OW) completed in the Coconino Sandstone also has negative sulfur isotopes where the groundwater shows reducing conditions next to a

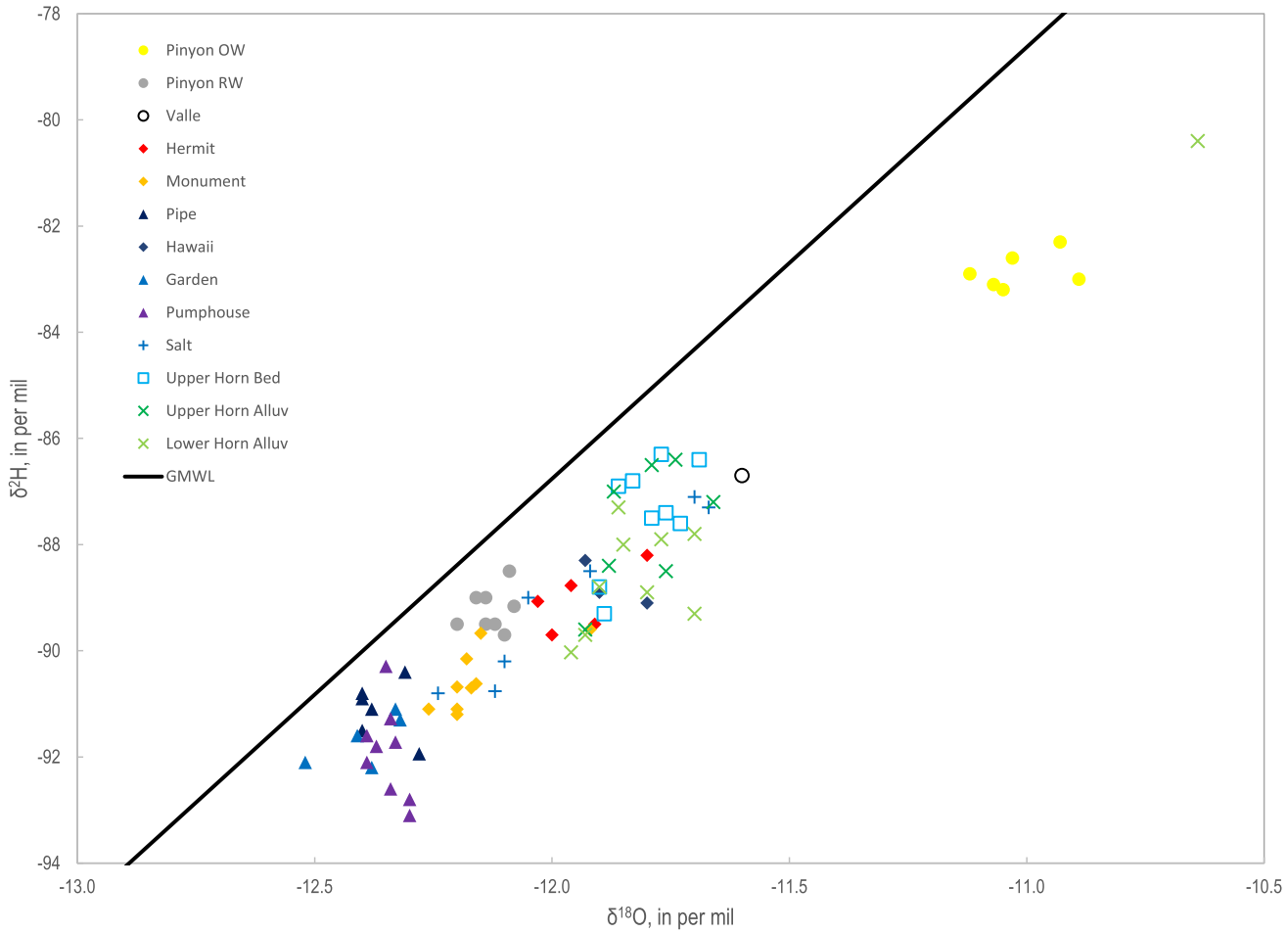

Fig. 6. Stable isotopic ratio of hydrogen (δ^2H) v. oxygen ($\delta^{18}O$) for groundwater samples (reported relative to Vienna Standard Mean Ocean Water (VSMOW)). Global meteoric water line (GMWL) from Craig (1961).

known mineralized breccia pipe, whereas the sulfur isotopic signature of the Pinyon Plain Regional Well (RW) completed in a deeper stratigraphic unit in the Muav Limestone is positive and the water has dissolved the oxygen present. Negative values indicate sulfate-reducing bacteria, sulfide oxidation, or interaction with pyrite minerals which may be related to water in contact with the sulfide minerals associated with breccia pipe uranium mines. Sulfur isotopic values from the Horn Alluvial springs are less negative compared with Upper Horn Bedrock Spring but still negative in comparison to other groundwaters of the region (Fig. 5).

Stable isotopes of oxygen and hydrogen of the water molecule provide an indication of the elevation and seasonality of recharge precipitation where more negative values suggest higher-elevation winter recharge. Stable isotopic signatures of springs in the Horn Creek watershed are less negative compared with Pumphouse and Gardens Springs and are generally more similar to Valle groundwater, Hermit and Hawaii Springs with some influence of a more enriched endmember similar to the Pinyon Plain OW (Fig. 6). One sample from Lower Horn Alluvial Spring in September 2015 has a more enriched isotopic signature (−10.64, −80.4 for $\delta^{18}O$ and δ^2H respectively; Fig. 6) that may represent localized precipitation recharging the alluvial material, although the general chemistry of the water was similar to other samples from the site. Two samples collected at Upper Horn Bedrock and Upper Horn Alluvium Springs in November and December 2021 had high barium concentrations and also show a positive shift of stable isotopic signature compared with the samples in the previous and subsequent spring season samples (Fig. 7), which suggests water source changes may occur over short periods of time. The Horn Creek samples plot between groundwater from the regional Redwall −Muav aquifer and the perched Coconino aquifer and show temporal variability with regard to stable isotopic values compared to other nearby groundwater resources, which suggests a more localized recharge component that may vary seasonally (Fig. 7). $\delta^{18}O$ in Salt Spring also shows temporal variability, although fewer samples have been collected from that site as from the other sites in the dataset. More frequent sampling from springs would help constrain the variability.

Strontium isotopes ($^{87}Sr/^{86}Sr$) provide evidence of water rock interactions, with the highest values (>0.714) in the Proterozoic basement rocks (Patchett and Spencer 2001; Crossey *et al.* 2006; Bills *et al.* 2007; Johnson *et al.* 2011) and lower values in Paleozoic sedimentary rocks (0.70756–0.71216; Monroe *et al.* 2005 and Bills *et al.* 2007). Upper Horn Bedrock Spring has a high strontium concentration and isotopic ratio in the range of Proterozoic basement rocks while springs emerging from the alluvium have lower strontium concentrations and isotopic ratios, although the isotopic ratio values are still higher than the range of Paleozoic sedimentary rocks (Fig. 8). Balboni *et al.* (2016) found a high strontium isotopic ratio (0.76288) from uraninite from the Orphan Mine, which may suggest interaction between uranium mineralizing fluid that moved through the Orphan pipe with Paleozoic basement rocks. However, there is debate regarding the source of mineralizing fluid in the breccia pipes of the Grand Canyon and high heterogeneity of mineralization within and between mineralized breccia pipes has been documented (Wenrich 1985; Huntoon 1996). Pipe Spring also has high strontium isotopic ratios which may indicate that water in the spring interacts with Proterozoic basement

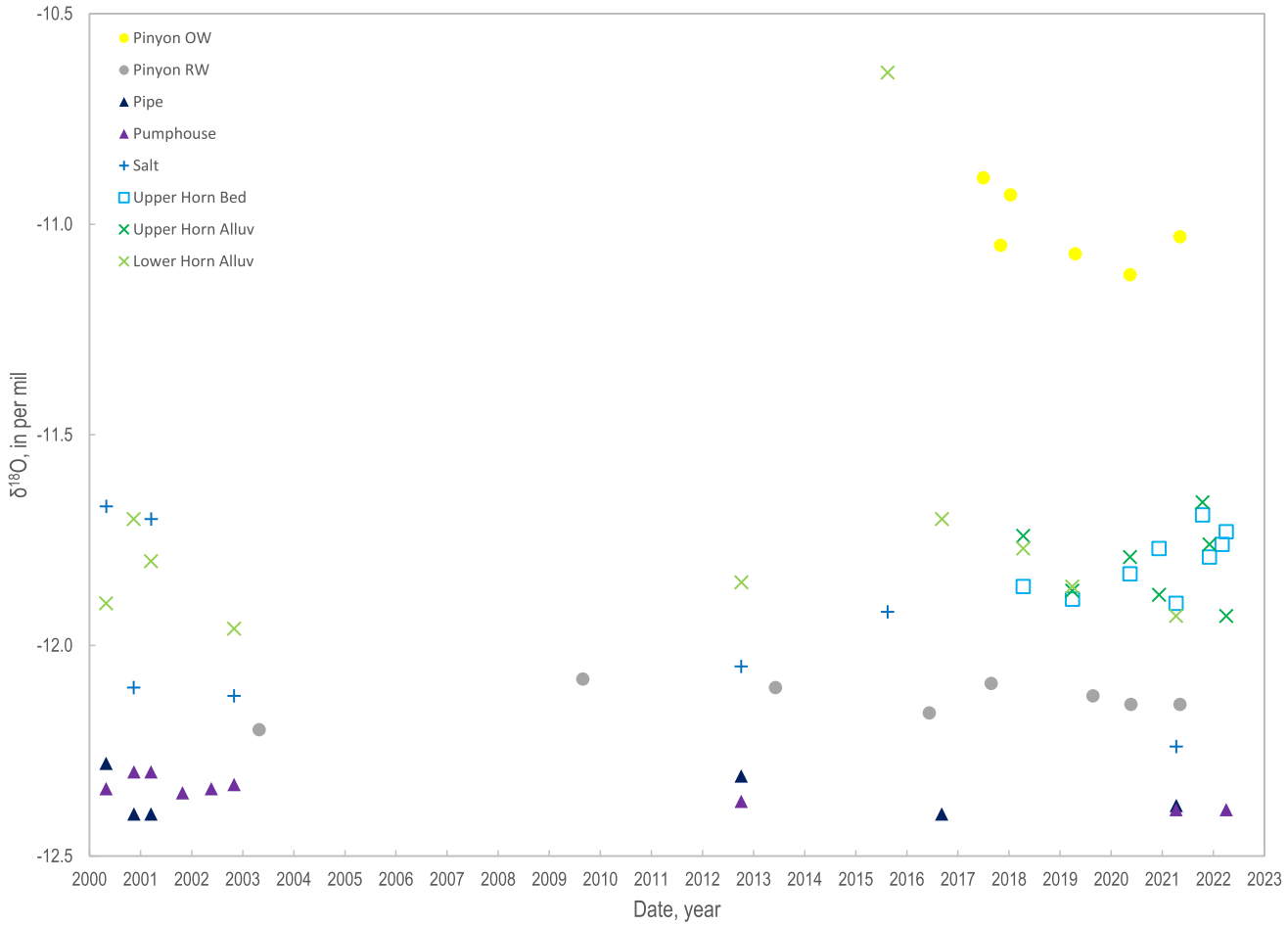

Fig. 7. Temporal variability of stable isotopic ratio of oxygen ($\delta^{18}O$) for groundwater samples.

rocks or a breccia pipe, although the uranium concentration at Pipe Spring is low compared with other sites in the area.

Groundwater age

Tritium is a tracer that indicates the presence of precipitation that fell after 1952 (Solder *et al.* 2020). Generally, tritium values for springs along the South Rim of Grand Canyon are low (less than 3 pCi l^{-1}) with some sites less than the laboratory reporting level (Garden Springs, Pumphouse Spring, Valle groundwater, Pinyon Plain OW and RW; USGS 2022). Tritium values in Horn Creek bedrock and alluvial springs were higher compared with surrounding springs and showed temporal variability. Tritium values were lower in the Upper Horn Bedrock Springs than in the springs emerging from the alluvium. In April 2019, all Horn Spring sites had the highest tritium values ever recorded, ranging from 5.04 to 7.78 pCi l^{-1}. Conversely, the concentration of uranium in the bedrock spring in April 2019 was the lowest measured during the study period, yet the opposite was the case for uranium in the lower alluvial spring (Fig. 9). The tritium data suggest changes in the component of modern water moving through the groundwater in Horn Creek. A better understanding of modern precipitation moving through the Orphan Mine workings could better characterize trace element mobilization of the remaining mining material.

Radiocarbon data provide information on the interaction of water with soil gas CO_2 and solid carbonate minerals as the water moves through the subsurface. Groundwater along the South Rim of Grand Canyon has mean groundwater ages of several thousand years (Solder *et al.* 2020). Garden and Pumphouse Springs have groundwater ages ranging from 2750 to 12 040 years and some springs with higher tritium values have lower mean ages, of which Horn Creek Spring (Lower Horn Alluvium) had the youngest mean age of 356 years (Solder *et al.* 2020). There is a large shift in the $\delta^{13}C$ (decrease of about 5 per mil) and ^{14}C (increase of about 30 percent modern carbon) between the Horn Upper Bedrock and Alluvial Springs (Fig. 10) suggesting water interacting with soil gas is influencing the carbon isotopes of alluvial springs. The evidence of interaction with soil gas plus an increase in tritium at the alluvial springs suggests the addition of water that recharged directly into the alluvial material of the Horn Creek watershed may be mixing with water discharging from the Upper Horn Bedrock Spring. Another possibility is that the water has undergone evaporation and interaction with soil gas in the alluvial material; however, the stable isotopic data do not suggest an evaporative signature between the bedrock and alluvial springs (Fig. 6).

Anthropogenic organic compounds

In 2021, two PFAS compounds (PFBA 6.0 ng l^{-1} and PFBS 1.5 ng l^{-1}) were detected above the laboratory detection level at the Horn Creek Upper Bedrock Spring site. Sampling was repeated in 2022 and values of the two compounds were <5.6 and <2.8 ng l^{-1} for PFBA and PFBS, respectively. The detections in 2021 may suggest some contribution of water in contact with anthropogenic materials in the mine workings or treated wastewater that is periodically recharged from Grand Canyon Village on the South Rim and moving through the mine workings. The latter hypothesis is being explored in a separate, more detailed study where no other pharmaceutical products typically found in treated wastewater were detected at Upper Horn Bedrock Spring (Beisner *et al.* 2023).

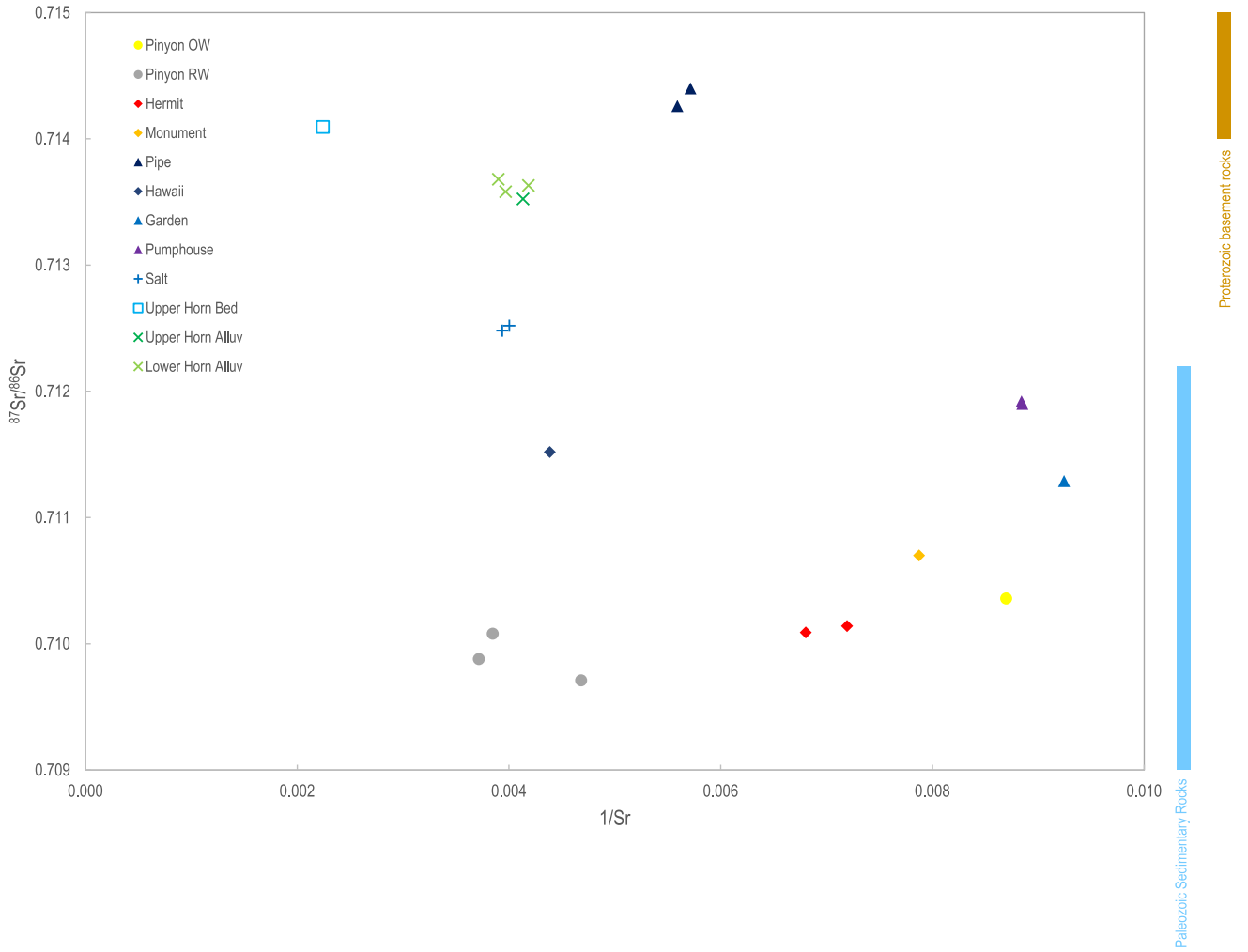

Fig. 8. Strontium isotopic ratio ($^{87}Sr/^{86}Sr$) v. inverse of strontium concentration for groundwater samples. Coloured bars on the right of the graph represent strontium isotopic concentration from geologic units (Patchett and Spencer 2001; Monroe *et al.* 2005; Crossey *et al.* 2006; Bills *et al.* 2007; Johnson *et al.* 2011).

Discussion

Uranium at Upper Horn Bedrock Spring is the highest observed concentration within groundwater samples of the watershed region surrounding Grand Canyon National Park (Tillman *et al.* 2021). The Orphan Mine is located in the upper reaches of the Horn Creek watershed above Upper Horn Bedrock Spring. The vertical shaft from the rim of the canyon has been sealed off, but there is an opening in the rock roof of Orphan Mine on the side of the cliff near the Coconino Sandstone stratigraphic unit that is open to the atmosphere and the mine workings and continues to widen and collapse. Additionally, there were exploratory holes drilled into the lowest levels of the mine workings that may provide pathways for water movement below the mine workings (Fig. 2). A relation between water moving through the Orphan Mine workings and Upper Horn Bedrock Spring is probable, but direct evidence of the connection through a tracer test could provide more concrete evidence than presented here.

The decrease in uranium concentration from Upper Horn Bedrock Spring to the Horn Alluvial Springs is likely the result of mixing with other waters that dilute the uranium concentration and/or through mineral precipitation or adsorption within the subsurface that preferentially removes the uranium. Several lines of geochemical evidence including specific conductance, strontium and uranium isotopes, and tritium suggest a dilution of the alluvial water. Bern *et al.* (2022) conducted laboratory experiments where they simulated native groundwater (deionized water interacted with Kaibab and Toroweap Formations and addition of gypsum and NaCl) interacting with breccia pipe uranium mining ore material (for one sample enriched in uranium and the other lower in uranium but elevated in many other trace elements), changed the redox environment, and simulated the interaction with sedimentary stratigraphic units that occur next to the breccia pipe down through the upper Muav Limestone. These experiments show little to no decrease in uranium concentration for the enriched uranium ore with concentrations around 200 000 μg l^{-1}. A decrease of around an order of magnitude was observed for the lower uranium ore (initial concentration of 1980 μg l^{-1}). The highest decreases were in water samples in contact with the Redwall Limestone, Esplanade Sandstone, upper Muav Limestone and Hermit Formation; there was only a minor decrease in uranium in contact with the Coconino Sandstone. Uranium concentrations at the end of the simulation for this lower-grade uranium ore were still an order to several orders of magnitude greater (20.6 to 694 μg l^{-1}; Bern *et al.* 2021) than the original simulated groundwater (0.536 μg l^{-1}). Simulated mine water did not interact with lower Muav Limestone or Bright Angel Shale which are present beneath the alluvium in Horn Creek. Minerals in the Muav Limestone and Bright Angel Shale including hematite, goethite and glauconite may help facilitate conditions for uranium and sulfate to precipitate in the subsurface.

Inverse modelling in PHREEQC (Charlton and Parkhurst 2002) was used to simulate Upper Horn Bedrock water interacting with mineral phases as it flows towards the Horn Alluvial Springs and

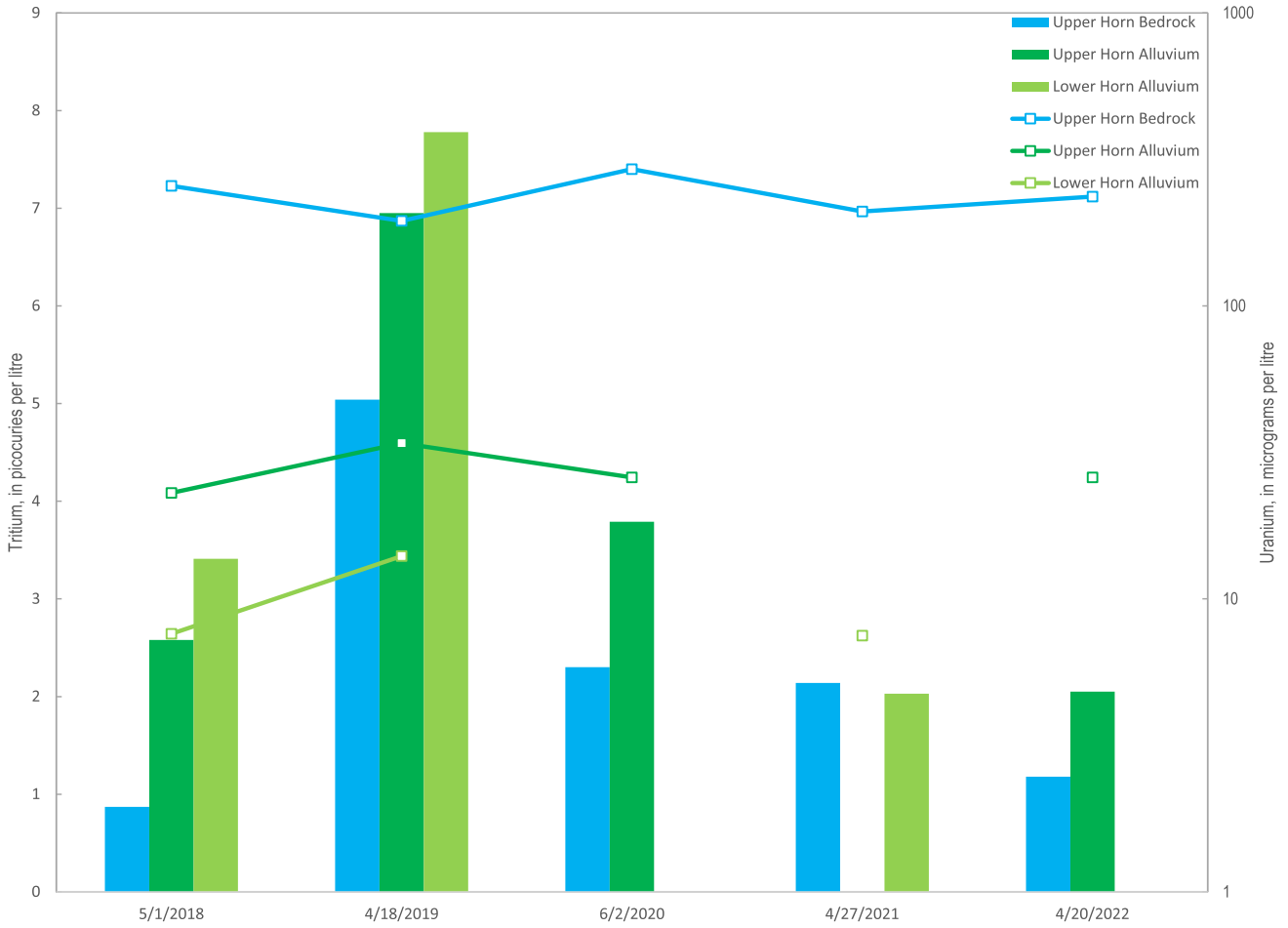

Fig. 9. Tritium (bars) and uranium (lines) for groundwater samples collected from 2018 to 2022 in Horn Creek.

mixing with other waters to assess what geochemical conditions are needed to produce the alluvial water (Beisner 2023). Mineral phases used in the simulations were based on geologic unit descriptions of stratigraphic units (Kaibab Formation, Toroweap Formation, Coconino Sandstone, Hermit Formation, Supai Group, Redwall Limestone and Muav Limestone; Beus and Morales 1990; Billingsley *et al.* 2008) that have eroded into the alluvial material of Horn Creek, from the Bright Angel Shale (Snelling 2021), and from the Orphan Mine deposit (Chenoweth 1986). Calcite, kaolinite, dolomite, hematite and gypsum were included in the geochemical simulations (Beus and Morales 1990; Billingsley *et al.* 2008). Quartz, dolomite and illite were included from the Bright Angel Shale (Snelling 2021). Uraninite, pyrite and gypsum were included in the system due to their presence in the breccia pipe (Chenoweth 1986), although it is unclear if these minerals would be present along the flow path between Upper Horn Bedrock Spring and the Horn Alluvial Springs. Resulting saturation indices for the waters used in the simulation are presented in Table 2 and suggest calcite and dolomite are near saturation, gypsum is slightly undersaturated, and halite, uranium oxide, uranium dioxide and uraninite are highly undersaturated.

Inverse modelling of Upper Horn Bedrock water from 2022 without mixing with other waters, only mineral phases, resulted in models that would need to dissolve calcite, kaolinite, quartz, $CO_2(g)$ and halite and precipitate gypsum, dolomite, illite and uraninite. Initial modelling included hematite and pyrite and produced one additional model with other phases the same as the previously described model and added hematite precipitating and pyrite dissolving (Table 3; Beisner 2023). Since the aqueous iron data from all Horn Creek groundwaters were highly variable with most values less than the reporting level (ranging from <0.3 to <18 $\mu g\,l^{-1}$) and all other values less than or equal to the highest laboratory reporting level and dissolved oxygen present, iron mineral phases were removed from subsequent model runs (USGS 2022). Iron mineral phases may be present in the Horn Creek Alluvial material and could cause trace element adsorption that may influence the trace element chemistry of waters moving past the iron minerals that may be separate from the bulk chemical changes being modelled in PHREEQC. Additionally, the uranium mineral phase (uraninite) was included in the PHREEQC model in order to balance the uranium concentration. However, if uraninite is present in the alluvial material it is likely unevenly distributed as would be the case for the iron minerals. Taking out the uraninite and the requirement for uranium to be balanced gives the same first model presented above that describes the overall change in chemistry of the major ions in the water. Local areas of reducing conditions within the alluvial material may also provide conditions to allow precipitation of uranium minerals, but these areas are not well characterized within the alluvium.

A mineral phase containing chloride is needed to account for the increase between the upper bedrock and alluvial waters and this modelling effort used halite, although it is not known to be prevalent in the stratigraphic units of the area. There are evaporite deposits in the Kaibab and Toroweap Formations that are known to have gypsum minerals, and perhaps other small amounts of other evaporite minerals are present or may form as water evaporates within the alluvial material. Sampling alluvial materials to determine iron, uranium and evaporite minerals and conducting batch experiments on alluvial material could help better characterize rock–water interactions in the watershed.

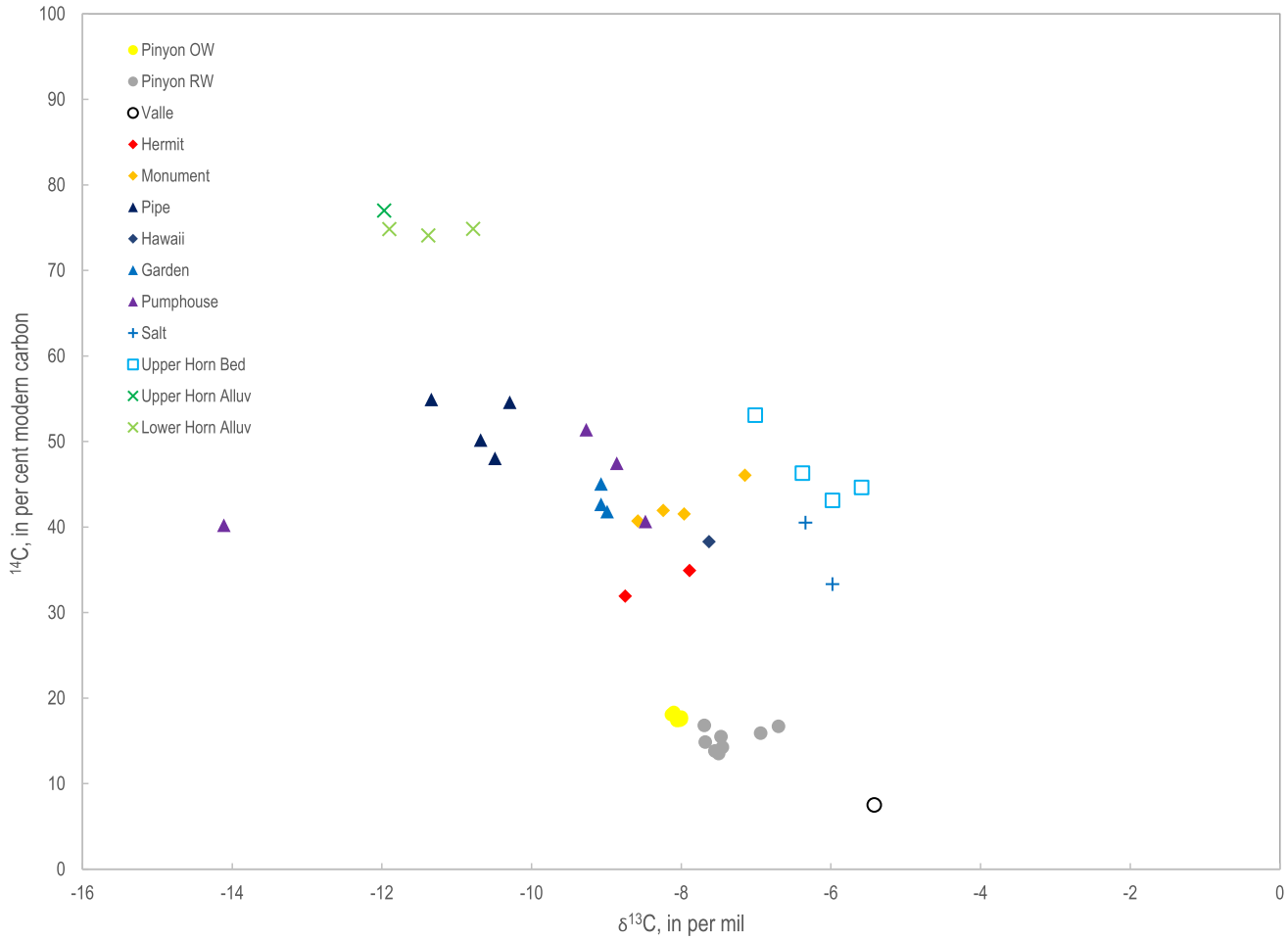

Fig. 10. Radiocarbon (^{14}C) v. carbon isotopic ratio ($\delta^{13}C$) for groundwater samples ($\delta^{13}C$ reported relative to Vienna PeeDee Belemnite (VPDB)).

The addition of other waters to the flow path between Upper Horn Bedrock and the Horn Alluvial groundwaters was also simulated in PHREEQC to understand relative proportions, suitability of endmember mixing waters and additional mineral interactions that would need to occur (Table 3; Beisner 2023). Addition of other waters between the bedrock and alluvial sites is supported by the qualitative increase in flow, decrease in specific conductance, decrease in uranium and other trace elements such as arsenic, and an increase in tritium. Additional waters to use as endmembers to mix with Upper Horn Bedrock were Pumphouse Spring (based on several lines of geochemical evidence that show Horn Alluvial groundwater plots between the two (Figs 3, 5, 6 and 8)) and Valle groundwater (which has geochemical values of isotopes of water and uranium and major ions similar to Horn Creek alluvial waters (Figs 3, 4 and 6) and elevated chloride compared with most other groundwaters of the region (Supplementary Information). However, both Pumphouse Spring and Valle groundwater have tritium below the laboratory reporting level, and do not contribute to the increase in tritium in the alluvial waters.

Table 2. *Saturation indices from PHREEQC (Beisner 2023)*

	Solution											
	1 UHB 2018	2 UHB 2019	3 UHB 2020	4 UHB 2022	5 UHA 2018	6 UHA 2019	7 UHA 2020	8 UHA 2022	9 LHA 2018	10 LHA 2019	11 PHS 2022	12 VGW 2004
Calcite	0.45	−0.18	−0.28	0.26	0.35	−0.22	0.45	0.09	−0.08	−0.35	−0.15	0.05
Dolomite	1.04	−0.29	−0.4	0.67	0.73	−0.36	1.04	0.2	−0.03	−0.56	−0.11	0.2
Gypsum	−1.26	−1.33	−1.29	−1.28	−1.69	−1.53	−1.63	−1.73	−1.81	−1.57	−2.69	−1.49
Halite	−8.04	−8.09	−8.07	−8.04	−7.73	−7.78	−7.78	−7.76	−7.71	−7.73	−8.77	−7.84
U_3O_8	−10.85	−8.8	−7.88	−10.31	−14.54	−11.68	−14.53	−13.34	−14.26	−12.33	−15.92	−13.19
UO_2	−12.1	−10.33	−10.34	−11.74	−12.69	−11.08	−13.42	−12.12	−12.36	−11.29	−13.46	−12.92
Uraninite	−7.7	−6.07	−5.8	−7.3	−8.34	−6.73	−8.66	−7.66	−7.93	−6.87	−8.7	−7.92
$CO_2(g)$*	−3.13	−2.52	−2.28	−2.9	−2.44	−1.99	−2.24	−2.1	−2.19	−1.91	−2.04	−1.92
$O_2(g)$*	−0.69	−0.78	−0.76	−0.76	−0.79	−0.82	−0.94	−0.83	−0.77	−0.77	−0.74	−0.92

UHB, Upper Horn Bedrock; UHA, Upper Horn Alluvium; LHA, Lower Horn Alluvium; VGW, Valle Groundwater; PHS, Pumphouse Spring.
*Values represent log10(fugacity). Fugacity = pressure × phi/1atm. For ideal gases, phi = 1.

Table 3. *PHREEQC inverse modelling results (Beisner 2023)*

Model Number	Percentage Initial Waters	Minerals Precipitating (mole transfers)	Minerals Dissolving (mole transfers)
2022 UHB reacting with mineral phases–UHA final water			
1	100% UHB	gypsum(-1.894×10^{-03}), dolomite (-7.348×10^{-04}), illite (-1.707×10^{-04}), hematite (-5.902×10^{-06}), uraninite (-8.829×10^{-07})	calcite (2.503×10^{-03}), kaolinite (1.963×10^{-04}), quartz (2.048×10^{-04}), halite (2.523×10^{-04}), pyrite (1.180×10^{-05}) CO_2(g) (1.594×10^{-03})
2	100% UHB	gypsum(-1.870×10^{-03}), dolomite (-7.348×10^{-04}), illite (-1.707×10^{-04}), uraninite (-8.829×10^{-07})	calcite (2.480×10^{-03}), kaolinite (1.963×10^{-04}), quartz (2.048×10^{-04}), halite (2.523×10^{-04}), CO_2(g) (1.618×10^{-03})
2022 UHB reacting with mineral phases–UHA final water (removed uranium balance, and uraninite, hematite and pyrite phases)			
1	100% UHB	gypsum (-1.870×10^{-03}), dolomite (-7.356×10^{-04}), illite (-1.707×10^{-04})	calcite (2.481×10^{-03}), kaolinite (1.963×10^{-04}), quartz (2.048×10^{-04}), halite (2.523×10^{-04}), CO_2(g) (1.619×10^{-03})
2022 UHB mixing with PHS–UHA final water (not including two models with 100% UHB or PHS)			
1	30% UHB 70% PHS	kaolinite (-8.476×10^{-05}), quartz (-8.845×10^{-05})	dolomite (2.338×10^{-04}), illite (7.371×10^{-05}), halite (4.701×10^{-04}), CO2(g) (9.153×10^{-04})
2	16% UHB 83% PHS	kaolinite (-1.396×10^{-04}), quartz (-1.457×10^{-04})	gypsum (2.869×10^{-04}), dolomite (2.747×10^{-04}), illite (1.214×10^{-04}), halite (5.449×10^{-04})
3	44% UHB 56% PHS	gypsum (-4.825×10^{-04})	calcite (8.676×10^{-04}), halite (3.983×10^{-04})
4	26% UHB 74% PHS	kaolinite (-1.001×10^{-04}), quartz (-1.045×10^{-04})	calcite (3.357×10^{-04}), dolomite (1.621×10^{-04}), illite (8.706×10^{-05}), halite (4.911×10^{-04})
5	32% UHB 68% PHS	kaolinite (-7.820×10^{-05}), quartz (-8.160×10^{-05})	calcite (4.427×10^{-04}), illite (6.800×10^{-05}), halite (4.612×10^{-04}), CO_2(g) (9.694×10^{-04})
2022 UHB mixing with VGW–UHA final water			
1	33% UHB 67% VGW	gypsum (-1.018×10^{-03}), dolomite (-1.562×10^{-04})	calcite (9.665×10^{-04})
2019 UHB mixing with VGW–UHA final water			
1	45% UHB 55% VGW	gypsum (-2.7854×10^{-04})	CO_2(g) (9.759×10^{-04})
2	38% UHB 62% VGW	gypsum (-2.7854×10^{-04}), kaolinite (-7.234×10^{-05}), quartz (-7.549×10^{-05})	illite (6.291×10^{-05})
3	45% UHB 55% VGW	gypsum (-4.335×10^{-04})	dolomite (2.164×10^{-04})
4	45% UHB 55% VGW	gypsum (-5.589×10^{-04})	calcite (3.822×10^{-04})

UHB, Upper Horn Bedrock; UHA, Upper Horn Alluvium; VGW, Valle Groundwater; PHS, Pumphouse Spring.

When water with chemistry from Pumphouse Spring in 2022 is simulated to mix with Upper Horn Bedrock Spring, five models fit the scenario with mixtures of 16–44% bedrock and 56–83% Pumphouse Spring water with phase mole transfers of calcite, gypsum, kaolinite, quartz, illite, halite, CO_2(g) and dolomite (Table 3; Beisner 2023). Simulations using Valle groundwater do not need to include the halite phase and result in one model run with 33% bedrock and 67% Valle groundwater with dissolution of calcite and precipitation of gypsum and dolomite.

Data from 2019 were also run with the same PHREEQC modelling inputs as 2022 data and resulted in three models with slightly different proportions of water, 45% bedrock to 55% Valle groundwater, and only gypsum precipitating and calcite, dolomite and CO_2(g) dissolving and one model with 38% bedrock to 62% Valle groundwater and gypsum, kaolinite and quartz precipitating and illite dissolving (Table 3; Beisner 2023).

Assuming the mixture percentages from the PHREEQC modelling and using the concentration of uranium from each mixing source, the resultant calculated uranium at the Upper Horn Alluvial Spring would be higher than what was observed (determined by summing the uranium concentration at each mixing source multiplied by the percentage of each source). The measured uranium concentration at Upper Horn Alluvial Spring in 2022 was 26 and 34 μg l^{-1} in 2019. The PHREEQC simulated mixing percentages resulted in calculated uranium concentrations of 39 to 98 μg l^{-1} in 2022, and 95 μg l^{-1} in 2019.

Addition of meteoric waters that fall as precipitation and infiltrate into the alluvial material likely occurs but may be seasonally variable. The pure water may dissolve mineral phases as it moves through the subsurface and the concentrations of the resultant water would be dependent on the reaction time and solubility of the mineral phases. The meteoric water component would add tritium to the water and dilute the trace elements associated with the Upper Bedrock Spring. It seems likely that the meteoric water component is in addition to another groundwater source due to the consistency of flow discharging from the alluvial material, lower measured uranium than predicted from modelled mixtures, chloride increase, and slight increase in tritium that is less than tritium in modern precipitation. Water storage capacity in the alluvial material of Horn Creek watershed is not well understood and further data could constrain relative contribution to the alluvial spring including temporal variability.

Decrease of uranium in water as it flows through the Horn Creek watershed is likely a result of dilution from mixing with waters of lower uranium concentration. Water resources near other mined breccia pipe uranium deposits of the region may accumulate elevated uranium concentrations and, as demonstrated in Bern *et al.* (2022), the uranium concentration is unlikely to decrease by interaction with surrounding sedimentary rock deposits. Conditions such as reductive zones, iron minerals, organic material or mixing with water of lower uranium concentration would be needed to decrease the uranium concentration as the water moved away from interaction with the mined breccia pipe.

Bacterially mediated uranium reduction is known to occur in natural environments and may also cause sequestration of uranium in the subsurface (Druhan *et al.* 2008; Basu *et al.* 2014; You *et al.* 2021). Microbial activity is often electron donor limited and is enhanced with the addition of organic compounds at bioremediation sites in areas of known uranium contamination (Druhan *et al.* 2008). However, You *et al.* (2021) suggest that reoxidation of uranium reduced by uranium-reducing bacteria may occur in environments with dissolved oxygen, nitrate and ferric iron. The groundwaters in this study, including those discharging within Horn Creek, have high concentrations of dissolved oxygen, suggesting conditions which would support uranium mobilization. Bacterially mediated

uranium reduction may be occurring in local subsurface environments within the study area, but overall oxic conditions suggest that bacterially mediated reduction would be a limiting factor in controlling uranium mobility in the groundwater of the Horn Creek watershed.

Conclusions

The Grand Canyon region contains breccia pipe deposits, some of which are mineralized and contain ore-grade copper and uranium. The Orphan Mine is an abandoned mineralized breccia pipe deposit that was mined for copper and uranium in the twentieth century and is located near the Horn Creek watershed. Uranium concentrations in the Horn Creek watershed of Grand Canyon are the highest values from groundwater in the Grand Canyon region. Water resources in contact with the Orphan Mine and potential interaction with waters in Horn Creek are not well understood. Additionally, the concentration of uranium decreases around an order of magnitude between groundwater emerging from the bedrock at the top of the watershed and the water emerging from the alluvial material lower in the watershed. This study assesses the geochemical tracers from Horn Creek water samples related to other nearby groundwater to determine anthropogenic changes and utilizes PHREEQC modelling to understand possible chemical interactions that are occurring in waters of Horn Creek.

The water chemistry of Horn Creek and Salt Creek groundwaters is anomalous compared to surrounding watersheds with higher sulfate and uranium concentrations. Sulfur and uranium isotopic ratio values are much lower compared with other groundwater in the region and suggest sulfide oxidation and interaction with uranium near secular equilibrium such as may occur with water interaction with sulfide and uranium minerals in mineralized breccia pipe deposits. Tritium is also elevated in Horn Creek groundwater, which suggests a higher component of water that fell as modern precipitation after the early 1950s, and some of this modern precipitation may have moved through the Orphan Mine workings then combined with other groundwater that would normally discharge in the Horn Creek watershed. PFBA and PFBS were found in low concentrations in the groundwater emerging from the bedrock at the top of the Horn Creek watershed and may be related to materials used in the mining process or other anthropogenic activities occurring nearby in Grand Canyon Village.

PHREEQC modelling suggests that elevated uranium water emerging from the bedrock at the top of the Horn Creek watershed may mix with other groundwater and precipitation that infiltrated into the alluvial material. Groundwater chemistry near Valle, AZ (located to the south of Horn Creek) is similar to the water emerging from the alluvial material in Horn Creek and also has elevated chloride that is not found in most other groundwaters in the Redwall–Muav aquifer of the region. The Valle groundwater was simulated to mix with the Upper Horn Bedrock groundwater and could account for more than half of the water in the alluvium. Horn Creek represents a system where elevated uranium water likely mixes with water containing lower uranium concentration. Additional studies could use dye or injected chemical tracers to build on this understanding of chemistry changes in the waters of Horn Creek as well as providing more direct evidence of contribution of water moving through the Orphan Mine.

Scientific editing by Carolina Rosca

Acknowledgements We would like to thank Benjamin Tobin, Robert Runkel and an anonymous journal reviewer for their suggestions to improve the paper. Any use of trade, firm or product names is for descriptive purposes only and does not imply endorsement by the U.S. Government.

Author contributions **KRB**: conceptualization (lead), data curation (lead), formal analysis (lead), funding acquisition (equal), investigation (lead), methodology (lead), project administration (equal), supervision (lead), writing – original draft (lead), writing – review & editing (lead); **CD**: conceptualization (supporting), formal analysis (supporting), writing – original draft (supporting), writing – review & editing (supporting); **FT**: funding acquisition (equal), project administration (equal), writing – review & editing (supporting).

Funding This research received funding from the U.S. Geological Survey Environmental Health Program (Toxic Substances Hydrology) and the U.S. Geological Survey-National Park Service Water Quality Partnership.

Competing interests The authors declare that they have no known competing financial interests or personal relationships that could have appeared to influence the work reported in this paper.

Data availability Data presented in this study are available through the USGS National Water Information System at https://doi.org/10.5066/F7P55KJN.

Correction notice Text on Fig. 2 updated.

References

Alpine, A.E. and Brown, K.M. 2010. Introduction. *In:* Alpine, A. (ed.) *Hydrological, Geological, and Biological Sites Characterization of Breccia Pipe Uranium Deposits in Northern Arizona. U.S. Geological Survey Scientific Investigations Report 2010–5025*, 1–16.

Balboni, E., Jones, N., Spano, T., Simonetti, A. and Burns, P.C. 2016. Chemical and Sr isotopic characterization of North America uranium ores: nuclear forensic applications. *Applied Geochemistry*, **74**, 24–32, https://doi.org/10.1016/j.apgeochem.2016.08.016

Ball, J.W. and Nordstrom, D.K. 1991. *Users WATEQ4F – User's Manual with Revised Thermodynamic Data Base and Test Cases for Calculating Speciation of Major, Trace and Redox Elements in Natural Waters*. U.S. Geological Survey Open-File Report **90–129**.

Basu, A., Sanford, R.A., Johnson, T.M., Lundstrom, C.C. and Loffler, F.E. 2014. Uranium isotopic fractionation factors during U(VI) reduction by bacterial isolates. *Geochemica et Cosmochimica Acta*, **136**, 100–113, https://doi.org/10.1016/j.gca.2014.02.041

Beisner, K.R. 2023. *PHREEQC Files for Geochemical Simulations in Horn Creek, Grand Canyon, AZ*. U.S. Geological Survey data release, https://doi.org/10.5066/P9X17FKG

Beisner, K.R., Paretti, N.V., Tillman, F.D., Naftz, D.L., Bills, D.J., Walton-Day, K. and Gallegos, T.J. 2017. Geochemistry and hydrology of perched groundwater springs: assessing elevated uranium concentrations at Pigeon Spring relative to nearby Pigeon Mine, Arizona (USA). *Hydrogeology Journal*, **25**, 539–556, https://doi.org/10.1007/s10040-016-1494-8

Beisner, K.R., Paretti, N.V., Jasmann, J.R. and Barber, L.B. 2023. Utilizing anthropogenic compounds and geochemical tracers to identify preferential structurally controlled groundwater pathways influencing springs in Grand Canyon National Park, Arizona, USA. *Journal of Hydrology: Regional Studies*, **48**, 101461, https://doi.org/10.1016/j.ejrh.2023.101461

Bern, C.R., Campbell, K.M., Walton-Day, K. and Keith, G.L. 2021. *Geochemical Data From Batch Experiments to Test Mobility of Trace Elements Downgradient from Breccia-Pipe Uranium Deposits*. U.S. Geological Survey data release, https://doi.org/10.5066/P9VILVZY

Bern, C.R., Campbell, K.M., Walton-Day, K. and Van Gosen, B.S. 2022. Laboratory simulation of groundwater along uranium-mining-affected flow paths near the Grand Canyon, Arizona, USA. *Mine Water and the Environment*, **41**, 370–386, https://doi.org/10.1007/s10230-022-00872-9

Beus, S.S. and Morales, M.J. 1990. *Grand Canyon Geology*. Oxford University Press, New York, NY.

Billingsley, G.H. 2000. *Geologic Map of the Grand Canyon 30′×60′ Quadrangle, Coconino and Mohave Counties, Northwestern Arizona. U.S. Geological Survey Geologic Investigations Series I-2688*.

Billingsley, G.H., Priest, S.S. and Felger, T.J. 2008. *Geologic Map of the Fredonia 30′×60′ Quadrangle, Mohave and Coconino Counties, Northern Arizona. U.S. Geological Survey Scientific Investigations Map 3035, scale 1;100,000*, https://pubs.usgs.gov/sim/3035/

Bills, D.J., Flynn, M.E. and Monroe, S.A. 2007. *Hydrogeology of the Coconino Plateau and Adjacent Areas, Coconino and Yavapai Counties, Arizona*. U.S. Geological Survey Scientific Investigations Report **2005–5222**, version 1.1, 101 pp, 4 plates, https://doi.org/10.3133/sir20055222

Bullen, T.D., Krabbenhoft, D. and Kendall, C. 1996. Kinetic and mineralogic controls on the evolution of groundwater chemistry and 87Sr/86Sr in a sandy silicate aquifer, northern Wisconsin. *Geochimica Cosmochimica Acta*, **60**, 1807–1821, https://doi.org/10.1016/0016-7037(96)00052-X

Charlton, S.R. and Parkhurst, D.L. 2002. *PHREEQCI-A Graphical User Interface to the Geochemical Model*. U.S. Geological Survey Fact Sheet PHREEQC **FS-031-02**.

Chenoweth, W.L. 1986. *The Orphan Lode Mine, Grand Canyon, Arizona: A Case History of a Mineralized, Collapse-Breccia Pipe*. U.S. Geological Survey Open-File Rep **86-510**.

Craig, H. 1961. Isotopic variations of natural waters. *Science*, **133**, 1702–1703, https://doi.org/10.1126/science.133.3465.1702

Crossey, L.J., Fischer, T.P., *et al.* 2006. Dissected hydrologic system at the Grand Canyon: interaction between deeply derived fluids and plateau aquifer waters in modern springs and travertine. *Geology*, **34**, 25–28, https://doi.org/10.1130/G22057.1

Druhan, J.L., Conrad, M.E., Williams, K.H., Guessan, L.N., Long, P.E. and Hubbard, S.S. 2008. Sulfur isotopes as indicators of amended bacterial sulfate reduction processes influencing field scale uranium bioremediation. *Environmental Science and Technology*, **42**, 7842–7849, https://doi.org/10.1021/es800414s

Faure, G. and Mensing, T.M. 2005. *Isotopes – Principals and Applications*. 3d edn. John Wiley & Sons, Inc., New Jersey.

Fitzgerald, J. 1996. *Residence Time of Groundwater Issuing from the South Rim Aquifer in the Eastern Grand Canyon*. MSc Thesis, University of Nevada, Las Vegas, NV, 103.

Garbarino, J.R. and Taylor, H.E. 1979. An inductively-coupled plasma atomic-emission spectrometric method for routine water quality testing. *Applied Spectroscopy*, **33**, 220–226, https://doi.org/10.1366/0003702794925732

Garbarino, J.R. and Taylor, H.E. 1996. *Inductively-Coupled Plasma-Mass Spectrometric Method for the Determination of Dissolved Trace Elements In Natural Water*. U.S. Geological Survey Open-File Rep **94-358**.

Huntoon, P.W. 1996. Large-basin ground water circulation and paleo-reconstruction of circulation leading to uranium mineralization in Grand Canyon Breccia Pipes, Arizona. *The Mountain Geologist*, **33**, 71–84.

Johnson, R.H., DeWitt, E., Wirt, L., Arnold, L.R. and Horton, J.D. 2011. *Water and Rock Geochemistry, Geologic Cross Sections, Geochemical Modeling, and Groundwater Flow Modeling for Identifying the Source of Groundwater to Montezuma Well, a Natural Spring in central Arizona*. U.S. Geological Survey Open-File Rep **2011–1063**.

Liebe, D. 2003. *The Use of the $^{234}U/^{238}U$ Activity Ratio at the Characterization of Springs and Surface Streams in Grand Canyon National Park, Arizona*. MSc Thesis, Hochschule fur Technik und Wirtschaft Dresden, Germany.

Monroe, S.A., Antweiler, R.C., Hart, R.J., Taylor, H.E., Margot, T., Rihs, J.R. and Felger, T.J. 2005. *Chemical Characteristics of Ground-Water Discharge Along the South Rim of Grand Canyon in Grand Canyon National Park, Arizona, 2000–2001*. U.S. Geological Survey Scientific Investigations Report **2004-5146**.

Ostlund, H.G., Rinkel, M.O. and Rooth, C. 1969. Tritium in the equatorial Atlantic Current system. *Journal of Geophysical Research*, **74**, 4535–4543, https://doi.org/10.1029/JC074i018p04535

Parkhurst, D.L. and Appelo, C.A.J. 2013. *Description of Input and Examples for PHREEQC Version 3: A Computer Program for Speciation, Batch-Reaction, One-Dimensional Transport, and Inverse Geochemical Calculations*. US Geological Survey Techniques and Methods, book 6, chap A43, USGS, Reston, VA.

Patchett, P.J. and Spencer, J.E. 2001. Application of Sr isotopes to the hydrology of the Colorado River System waters and potentially related Neogene sedimentary formations. *In:* Young, R.A. and Spamer, E.E. (eds) Colorado River Origin and Evolution: Proceedings of a Symposium, June 2000, Grand Canyon National Park, Arizona.

Révész, K. and Coplen, T.B. 2008*a*. *Determination of the δ2H/1H, of Water – RSIL Lab Code 1574*. US Geological Survey Techniques and Methods, book 10, chap. C1.

Révész, K. and Coplen, T.B. 2008*b*. *Determination of the δ18O/16O of Water – RSIL Lab Code 489*. U.S. Geological Survey Techniques and Methods, book 10, chap. C2.

Révész, K., Qi, H. and Coplen, T.B. 2012. *Determination of the δ 34S of sulfate in water; RSIL lab code 1951, chap. 10 of Stable isotope-ratio methods, sec. C of Révész, Kinga, and Coplen, T.B. eds., Methods of the Reston Stable Isotope Laboratory (slightly revised from version 1.1 released in 2007)*. U.S. Geological Survey Techniques and Methods, book 10, http://pubs.usgs.gov/tm/2006/tm10c10/

Shoemaker, J. and Tettenhorst, D. 2018. *Method 537.1: Determination of Selected Per- and Polyfluorinated Alkyl Substances in Drinking Water by Solid Phase Extraction and Liquid Chromatography/Tandem Mass Spectrometry (LC/MS/MS)*. U.S. Environmental Protection Agency, Office of Research and Development, National Center for Environmental Assessment, Washington, DC.

Snelling, A. 2021. The petrology of the bright angel formation, Tonto Group, Grand Canyon, Arizona. *Answers Research Journal*, **14**, 303–415, https://answersresearchjournal.org/petrology-bright-angel-tonto-group/

Solder, J.E., Beisner, K.R., Anderson, J.R. and Bills, D. 2020. Rethinking groundwater flow on the South Rim of the Grand Canyon, USA: characterizing recharge sources and flow paths with environmental tracers. *Hydrogeology Journal*, **28**, 1593–1613, https://doi.org/10.1007/s10040-020-02193-z

Taylor, H.E. 2001. *Inductively Coupled Plasma-Mass Spectrometry*. Academic, New York.

Thatcher, L.L., Janzer, V.J. and Edwards, K.W. 1977. *Methods for Determination of Radioactive Substances in Water and Fluvial Sediments*. *Techniques of Water-Resources Investigations of the U.S. Geological Survey*, book 5, chap. A5, 79–81, https://doi.org/10.3133/twri05A5

Tillman, F.D., Beisner, K.R., Anderson, J.R. and Unema, J.A. 2021. An assessment of uranium in groundwater in the Grand Canyon region. *Scientific Reports*, **11**, 22157, https://doi.org/10.1038/s41598-021-01621-8

U.S. Geological Survey. Variously dated. *National Field Manual for the Collection of Water-Quality Data*. *U.S. Geological Survey Techniques and Methods of Water-Resources Investigations*, book 9, chapt. A1–A10, http://pubs.water.usgs.gov/twri9A [last accessed 22 October 2022].

U.S. Geological Survey 2022. *USGS Water Data for the Nation*. *U.S. Geological Survey National Water Information System database*, https://doi.org/10.5066/F7P55KJN [last accessed 22 October 2022].

Wenrich, K.J. 1985. Mineralization of breccia pipes in Northern Arizona. *Economic Geology*, **80**, 1722–1735, https://doi.org/10.2113/gsecongeo.80.6.1722

You, W., Peng, W., Tian, Z. and Zheng, M. 2021. Uranium bioremediation with U(VI) -reducing bacteria. *Science of the Total Environment*, **798**, 149107, https://doi.org/10.1016/j.scitotenv.2021.149107